Enhanced cell wall mechanics in VirtualLeaf enable realistic simulations of plant tissue dynamics

Großeholz, R.; Nieuwenhoven, W.R. van; Mele, H.B.; Merks, R.M.H.

Journal Title Here, 2024, 1–13
doi: DOI HERE
Advance Access Publication Date: 26 Juli 2024
Paper

Enhanced Cell Wall Mechanics in VirtualLeaf Enable Realistic Simulations of Plant Tissue Dynamics

Ruth Großeholz[1,2,3] Richard W. van Nieuwenhoven[4,*] Bruno Hay Mele[5] and Roeland M.H. Merks[6,7]

[1]BioQuant, Heidelberg University, Heidelberg, Germany, [2]Maastricht Centre for Systems Biology, Maastricht University, Maastricht, Netherlands, [3]Brightlands Future Farming Insitute, Maastricht University, Venlo, Netherlands, [4]Institute of Applied Physics, TU Wien, Vienna, Austria, [5]Department of Biology, University of Naples, Naples, Italy, [6]Mathematical Institute, Leiden University, Leiden, Netherlands and [7]Institute for Biology Leiden (IBL), Leiden University, Leiden, Netherlands

*Corresponding author. nieuwenhoven@iap.tuwien.ac.at

FOR PUBLISHER ONLY Received on Date Month Year; revised on Date Month Year; accepted on Date Month Year

Abstract

Computational modelling has become increasingly important in advancing our understanding of biological systems, necessitating the development of new computational approaches and software. VirtualLeaf, in particular, is a modelling framework for plant tissues that accounts for the biophysical mechanics of plant cell interactions. The plant cell wall plays a pivotal role in plant development and survival, with younger cells generally having thinner, more flexible (primary) walls than older cells. Signalling processes in growth and pathogen infection also affect cell wall stability. This article presents an updated version of VirtualLeaf with improved cell wall mechanics and morphing behaviour. These are crucial for ultimately understanding plant tissue dynamics and essential signalling processes during growth, tissue formation and pathogen defence. The updated version of VirtualLeaf enables detailed modelling of variations in cell wall stability to the level of individual cell wall elements. These improvements lay the groundwork for using VirtualLeaf to address new research questions, including the structural implications of pathogen infection and growth.

Key words: cell-based modelling, VirtualLeaf, growth simulation software, plant tissue simulations

Introduction

Computational modelling has become an indispensable tool in biological research, irrespective of the area of research (Hübner et al., 2011; Rutten and ten Tusscher, 2019; Holzheu and Kummer, 2019). The increasing utilisation of computational modelling prompts the continuous development and refinement of modelling tools and software as new research questions arise. In terms of modelling software, several cell-based modelling packages have been developed: PhysiCell, which uses centre-based modelling of cells, is designed for simulating multicellular systems with a focus on cancer, tissue growth, and immune responses (Ghaffarizadeh et al., 2018); CompuCell3D is used for morphogenesis simulations in various biological contexts (Swat et al., 2012); Morpheus allows for modelling and simulation of multiscale and multicellular systems (Starruß et al., 2014); and the Tissue Simulation Toolkit (TST) supports simulation of cellular behaviour and tissue development (Merks and Glazier, 2005), with recent versions focusing in particular on detailed modelling of cell-extracellular matrix interactions. CompuCell3D, Morpheus, and TST are based on the Cellular Potts model.

Focusing specifically on plant tissue simulation, VirtualLeaf was developed to simulate plant tissues, emphasising cell mechanics (Merks et al., 2011). In contrast, alternatives such as MorphoDynamicX focus on the whole tissue shape, leading to individual cell behaviour (Chickarmane et al., 2010). VirtualLeaf, on the other hand, has an in-depth 'cell-based' approach where tissue shape emerges from the collective behaviour of individual cells.

VirtualLeaf is an open-source cell-based simulation software that supports analysis of cellular signalling and gene expression activity in the (plant) tissue context (Merks et al., 2011; Antonovici et al., 2021). It has been used to, e.g., study organ patterning in the floral meristem (van Mourik et al., 2012) or the pattern of root elongation (De Vos et al., 2014). Over time, VirtualLeaf was extended with functionalities to drive specific research questions, such as the concerted action of signalling and biophysics as drivers of plant tissue organisation (Lebovka et al.,

2023) and adhesion-driven cell sorting in animal epithelia (Wolff et al., 2019).

It is crucial to consider the specific characteristics of plant morphology when analysing computational models of plant tissues: plant tissue development and integrity rely in part on the precise regulation of cell wall stability and properties (Rui and Dinneny, 2019; Wolf, 2022). On the one hand, the cell wall needs to be more flexible during growth to allow cellular growth (Wolf et al., 2012). On the other hand, excessive cell wall weakening can compromise plant integrity, rendering the plant susceptible to pathogen infections. Generally, cell wall properties vary significantly between cell types and between older and younger cells — younger cells have thin, more flexible (primary) cell walls (Cosgrove, 1997). In comparison, older cells acquire thicker, more stable (secondary) cell walls over time (Li et al., 2016). The composition of the cell wall is influenced by multiple factors, such as the age of the cell and its biophysical properties (Freshour et al., 1996).

Various signalling pathways affect cell wall stability. During growth, both brassinosteroid (BR) and auxin signalling pathways can induce cell wall swelling and loosening (Wolf et al., 2012) as part of the preparatory steps for i.e. root growth (Caesar et al., 2011). The cell wall's mechanical properties change continually during vein formation in plants. Furthermore, the tissue cell polarity is tightly regulated during vein formation, resulting in structured xylem and phloem differentiation from vascular cambium (Mäkilä et al., 2023; Verna et al., 2019). BRs and auxin indirectly activate expansins *via* stimulating proton pump activity that causes the acidification of the cell wall (Caesar et al., 2011; Hager et al., 1971, 1991; Shcherban et al., 1995; Park and Cosgrove, 2012). Expansins, in turn, loosen the cell wall at cellulose-xyloglucan junctions, allowing the cells to expand (McQueen-Mason et al., 1992; Shcherban et al., 1995; Park and Cosgrove, 2012).

Plant physiological processes can likewise increase the stability of the cell wall. In response to elevated mechanical stress, such as intensified wind forces, plants adapt by augmenting cell wall thickness to enhance overall structural stability (Gall et al., 2015). The stability of the cell wall increases upon detecting pathogens (Ikeuchi et al., 2013), as the cell wall acts as a mechanical barrier that pathogens must overcome to become transmissible between cells (Hématy et al., 2009; Underwood, 2012). When a pathogen is detected, this triggers a wave of Ca^{2+} and reactive oxygen species (ROS) along the plant tissue, resulting in a more stable interaction between cell wall filaments. In response, pathogens evolved several different mechanisms by which they compromise cell wall stability, e.g. secretion of cell wall degrading enzymes by plant-pathogenic fungi (Kubicek et al., 2014; Rai et al., 2015). This evolutionary race has resulted in fierce competition between pathogens and plants, with pathogens developing new mechanisms to destabilise plant cell walls to outpace the plant's defence mechanisms (Bellincampi et al., 2014).

All these examples highlight the crucial role of cell wall dynamics and changes thereof to plant survival, growth, and development processes. Understanding these processes at different spatial scales — such as tissue- or organ-level — will require a reflection of the biophysical aspects arising from cell wall properties. As spatial scales increase, the complexity of these processes also grows, making them challenging to analyse comprehensively. Consequently, computational modelling has become an indispensable tool for understanding signalling networks in the context of a specific tissue or organ (De Vos et al., 2014; Lebovka et al., 2023). Several recent advances in plant research result from interdisciplinary studies combining an iterative cycle of experiments and computational simulations, such as in recent studies (Großeholz et al., 2022; Holzheu et al., 2021).

Here, we present an updated version of VirtualLeaf that implements a more fine-grained mechanical representation of the cell wall, allowing for cell-specific wall stability values. The fine-grained mechanical representation enabled the implementation of cell wall remodelling. These enhanced implementations pave the way for the use of VirtualLeaf in areas of research where cell wall stability and integrity play a prominent role, e.g. the mechanical effects of pathogen infection.

Methods

Simulations in VirtualLeaf

In VirtualLeaf, cells are represented as polygons composed of a series of nodes connected by springs (Fig. 5b). Tissues are then formed by connecting cells into meshes. Adjacent cells share their nodes and springs ensuring their relative position cannot change, except by specific moves. A Hamiltonian operator represents the tissue's mechanical energy. This Hamiltonian comprises the compression of cells and the stretch/resistance of the cell wall, and it can be expanded to include other relevant elements, such as cell stiffness or a target cell length. All the continuous dynamics (intracellular substances dynamics and diffusion) are described using a set of differential equations (ODE submodel). In contrast, an Individual-Based model (IBM submodel) controls cell differentiation and division. The IBM defines which Ordinary Differential Equations (ODEs) are active in the cell and regulates the diffusive term in the PDEs. The continuous and IBM submodels contribute to the Hamiltonian that controls cell spatial properties (such as area, perimeter, and shape), which, in turn, influence intracellular properties. Formulating the model in this way permits the definition of a hybrid model that operates across multiple time and space scales while coupling biochemical and mechanical dynamics.

VirtualLeaf represents cells in tissues as a dynamic mesh of non-overlapping polygons based on circular series of nodes. For every cell, it is possible to calculate an "internal energy" (H) that represents the balance between turgor pressure and wall tension. Generally, H is assessed using a Hamiltonian operator (Eq. (1)), summarising the effects of cell compression and cell-wall stretching. ΔA represents the area change and ΔL the change in wall length.

The Hamiltonian is composed of a contribution due to area conservation (A), and wall elasticity (L).

$$\Delta H = H_{\mathrm{A}} + H_{\mathrm{L}}. \tag{1}$$

The area conservation contribution describes the cell's turgor pressure and ensures the balance between cellular pressure and the pressure from the surrounding tissue (Merks et al., 2011). It is defined as the sum of squared deviations of cell areas ($A(i)$) with respect to a resting area ($A(i)_t$), weighted by a user-defined parameter (λ).

$$H_{\mathrm{A}} = \Sigma_i \lambda_i (A(i)_t - A(i))^2 \tag{2}$$

Wall elements, i.e. the wall segment between two nodes, are considered mechanical springs, with a resting length $L(j)_t$ and a specific spring constant λ_j:

$$H_{\mathrm{L}} = \lambda_j \Sigma_j (L(j)_t - L(j))^2. \quad (3)$$

The formulation is conceptually identical; however, this formula uses the wall element's length instead of the cell area.

For a detailed introduction to the computational approach taken in VirtualLeaf we refer to the following papers and book chapters: Merks et al. (2011) and Antonovici et al. (2021).

Tissue simulations

For the tissue simulations included in this manuscript, VirtualLeaf was compiled on a local computer. The model files and tissue XML files are included in the new release of VirtualLeaf; specifically, the lateral root model utilises the LateralRoot.xml template, and the infection model utilises the pathogen_infection.xml file. The simulation results (both XML files and movies) are available as supporting information.

Ensuring Backwards Compatibility

The auxin growth model was simulated ten times in both the 2021 release (Antonovici et al., 2021) and the version presented here utilising the new compatibility mode to test backwards compatibility (see Section 1.2.1). The compatibility mode allows for the use of previous implementations of the Hamiltonian. As implemented in R, the resulting cell counts and cell area values were compared using the Kolmogorov-Smirnov test.

Results

Initial Tissue Configuration (SVG translator)

In silico experiments on tissue development, the initial state of the tissue must be defined, and this has to be specific to the research question. In VirtualLeaf, tissues are represented by a dynamic mesh of nodes used to define walls, and cells are represented by non-overlapping polygons on the same mesh. VirtualLeaf utilises an XML template that can be manually modified to simulate the desired starting configuration. XML data adaptation is a tedious process and, in this specific case, requires meticulous attention to ensure an accurate definition of cell wall traversal over shared nodes. The updated version of VirtualLeaf was enhanced by incorporating a stand-alone, command-line SVG importer that can be used independently of VirtualLeaf. The importer facilitates the creation of the initial cell configuration through a user-friendly graphical interface, allowing users to model the cell's spatial arrangement in the tissue visually. Thanks to the SVG importer, it is possible to streamline the domain definition phase, allowing the user to focus more on the definition of biological processes.

The SVG file format is an XML-based file format; as such, it is efficiently readable by any XML parser. The way cells are defined in VirtualLeaf is remarkably similar to SVG syntax, e.g. the definition of a "cell" in VirtualLeaf is very close to those of the SVG "path" element, as both are defined as lines following a list of individual points. Cell attributes can be encoded in SVG, e.g. the path colour can be mapped to the cell type through the command line. There are a few constraints, like the inability to define curved walls, as they are not permitted in VirtualLeaf. Any information related to curvature is dropped — only points are imported. VirtualLeaf cells must have closed walls, which implies that every SVG path must be closed — for any open-ended path, the system will force the closure by connecting the first and last points of the path. Two nodes that are "close" (i.e. 0.75% of the image size) to each other are merged into one single node in VirtualLeaf. Two nodes that are "close" (i.e. 0.75% of the image size) to each other are merged into one single node in VirtualLeaf. For detailed instructions on preparing the SVG image and using the SVG importer we refer the readers to the supporting information.

Cell wall "remodelling"

While cell wall integrity and stability play an integral part in plant development and survival, there are circumstances during a plant's life cycle where localised growth necessitates the remodelling of the tissue, e.g. during lateral root emergence (Stoeckle et al., 2018) and during nodule development (Brewin, 2004). To implement this in VirtualLeaf we need to allow for an additional kind of "movement" during tissue simulations 2. Nodes still "wiggle" around to find a new, energetically more favourable position, as in previous versions of VirtualLeaf. To allow wall elements to "slide" to a more favourable node connection, we adopt a similar 'sliding' operator as previously proposed for modelling animal tissues (Wolff et al., 2019): In Fig. 3a, the geometry depicted results from the concurrent expansion of neighbouring cells along the outer border of the tissue domain and the discretisation caused by wall elements. This interaction produces a distinctive structure, characterised by sharp spikes that point inward or outward. By "sliding" the **b** wall element one node outward by one node — thereby connecting it to **c** rather than **d** — the energetic tension in the simulation model is reduced, producing a more realistic transition.

The stiffness redistribution, after each cell wall remodelling, along a cell wall is described by Eq. (4). The rule imposes where the stiffness (δ) per wall-element length (l) is kept constant (λ). During redistribution only the wall elements that have been newly introduced or were changed in length and their adjacent wall elements are updated while keeping λ constant (for example in **cell-1** in Fig. 3e the wall elements **a**, **b**, **d** and **c** get a recalculated wall stiffness.

$$\sum_{wall-element} \delta \times l = \lambda \quad (4)$$

A separate Monte Carlo step was introduced before cell housekeeping — the routines that update the simulation-specific cell status — and after the Monte Carlo node displacement to evaluate each wall element's remodelling energy change. Unlike the approach taken by Wolff et al. (2019), however, this second Monte Carlo step is based on the wall elements and the Hamiltonian for wall remodelling is based on the spring energy in the wall elements. The wall between two cells on both sides of the remodelled wall changes in opposite directions, resulting in Eq. (5).

$$H_{\mathrm{L}} = H_{\mathrm{elongated-L}} - H_{\mathrm{shortend-L}} \quad (5)$$

In cases where potential wall remodelling involves identical nodes, the remodelling is limited to one randomly but favours energetic equilibrium. The execution and selection of the wall remodellings are addressed during cell housekeeping, where cell division and growth processes occur. The diverted execution is due to cell neighbours and cell walls being repaired after this step. We have included the possibility for cells to "veto" cell wall remodelling by deactivating specific wall remodellings or setting the cell's property *veto_remodelling*. Specific cells or cell types

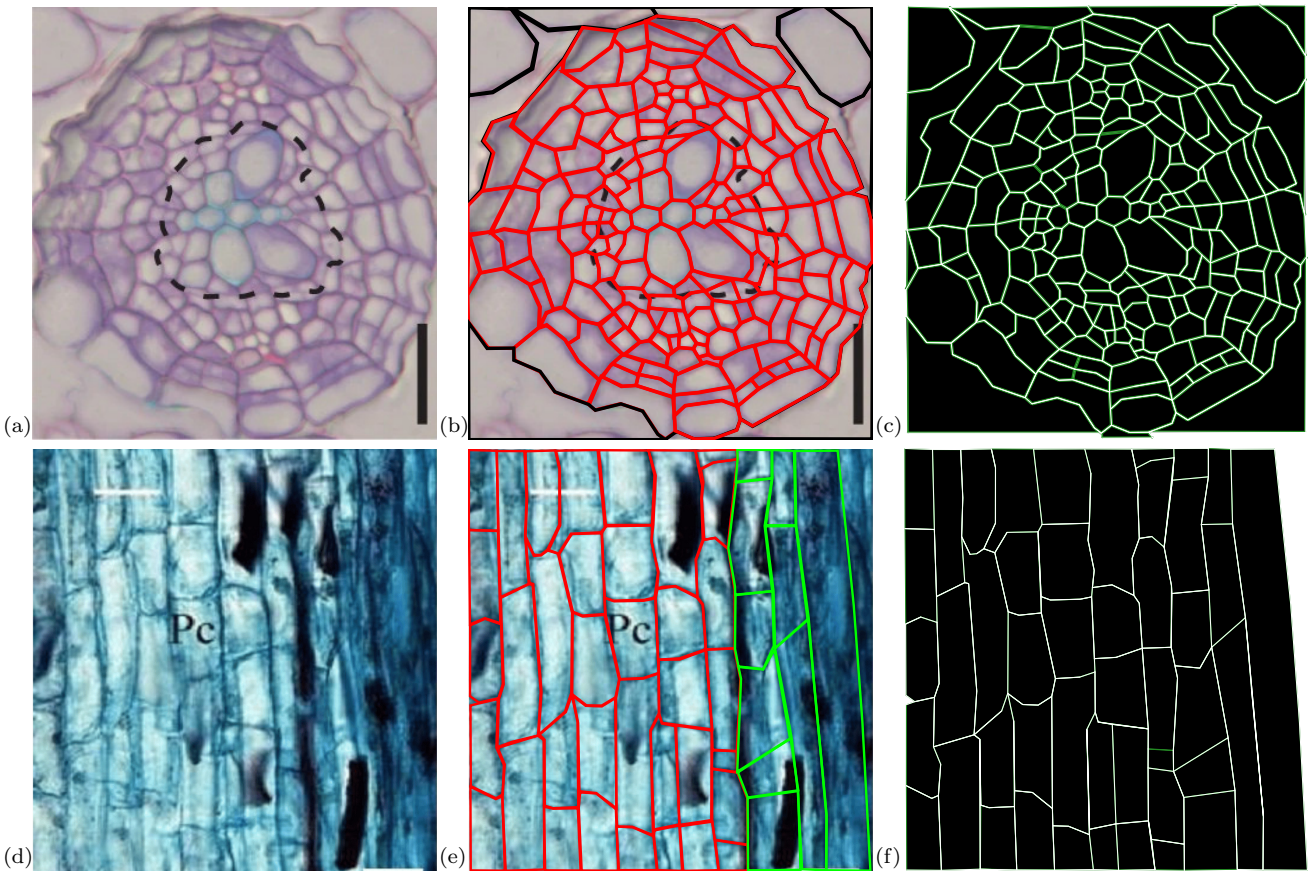

Fig. 1: Representation of the process of tissue modelling in three stages, from microscope image to VirtualLeaf XML tissue data. (a) initial microscope image of plant tissue section from (Mäkilä et al., 2023). (b) The SVG drawing was produced with Inkscape Harrington (2004-2005), keeping Fig. 1a as the background image. (c) SVG drawing Fig. 1b converted to VirtualLeaf XML tissue. The black outlined cells are border cells fixed in place for the simulation. (d) initial microscope image of longitudinal plant tissue (procambium) from Xu et al. (2023). (e) The SVG drawing was produced with Inkscape Harrington (2004-2005), keepingFig. 1d as the background image. Xylem cells (Green) are differentiated from procambium cells (red), giving structural integrity to the vessel wall. (f) SVG drawing Fig. 1e converted to VirtualLeaf XML tissue.

can be excluded from or included in cell wall remodelling. This property is accessible through the model in cell housekeeping and can change throughout the simulations. All cells sharing the remodelled cell walls can “veto” the remodelling individually.

The cell wall remodelling implementation has the additional advantage of avoiding tissue conformation artefacts that arose during simulations: In the classic VirtualLeaf framework, the segmentation of cell wall in wall elements can also cause artificial protrusions of the cytoplasm of a cell if it experiences compression for opposing sides as in the case of three cells sharing a single wall endpoint (see **cell-3** in Fig. 3b), forming a pointed end in the cell wall of **cell-3**. *In planta*, these sharp angles will only occur on a temporary basis during lateral root emergence, though this is only temporary as extensive cell wall remodelling will allow lateral roots to emerge (Stoeckle et al., 2018). The implementation of cell wall remodelling prevents these artefacts in VirtualLeaf and is named after the actual plant physiological process. This cell wall remodelling is parameterised based on cell wall properties. As in real systems, these properties are related to cell wall stiffness, varying according to both developmental stage and cell type. Handling the squished edge artefact in the different scenarios requires the same formal approach (from the algorithm standpoint, ”outside” in Fig. 3b and **cell-3** in Fig. 3a pose the same problem) i.e. the fusion of cell walls along the periphery.

Due to these enhancements, VirtualLeaf can now simulate plant tissue growth and development at a greater level of detail, allowing for the realistic remodelling of cell wall elements and generating growth patterns that mimic those observed in biological systems more closely.

New research direction: lateral root emergence

While cell wall stability is fundamental to plant stability and survival, there are instances during plant development in which the cell wall is actively remodelled. This happens, for instance, during lateral root emergence, where the new lateral root needs to push through the epidermis (Stoeckle et al., 2018). The example model illustrates this process within a simplified framework (Section 1.1.1). In the simulation, a single cell is designated as the founder cell initiating the lateral root. For the sake of simplicity, only this cell undergoes growth, and upon division, the daughter cell furthest to the right assumes the role of the new initiator.

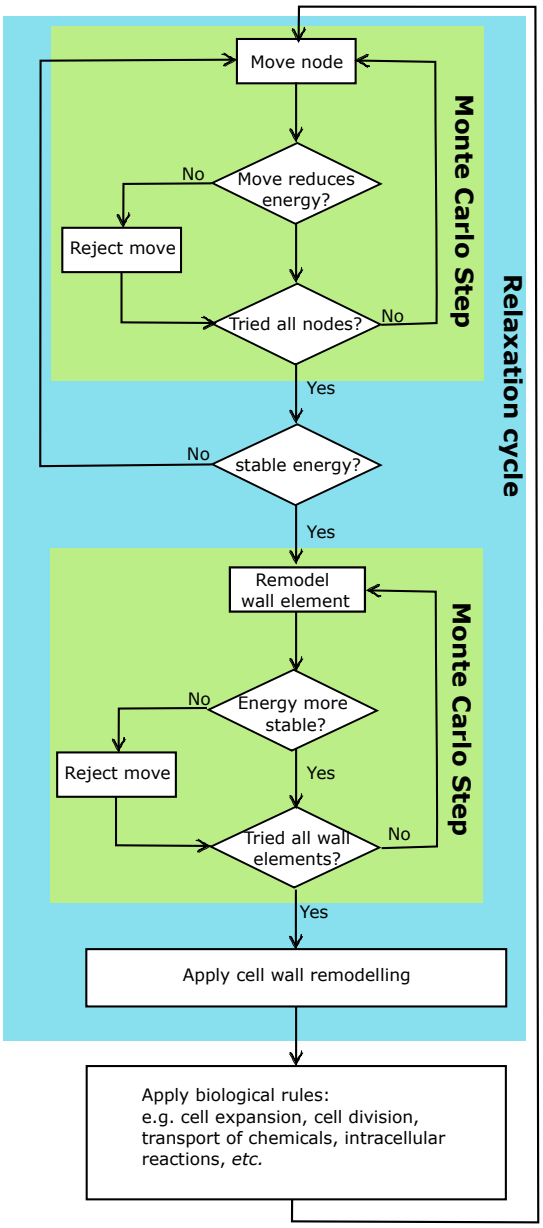

Fig. 2: Updated overview of the simulation steps. After the Monte Carlo step for node displacement, there is a second Monte Carlo step assessing all cell walls per node w.r.t. cell wall remodelling.

This minimal condition suffices to generate a structure resembling a lateral root.

Dynamic wall-element remodelling allows cell walls to adjust by shifting between nodes, evading pressure from neighbouring cells. By facilitating these adjustments, cell wall remodelling prevents the formation of cell shapes that are energetically unfavourable and unlikely to occur naturally. Wall-element remodelling allows cells to squeeze between other cells if energetically profitable, for example, supported by the pressure of a growing tissue cluster (Section 1.1.1). The video in the supplementary section Section 1.2.1 shows a more derailed evolution of the time-lapse represented in Section 1.1.1. This mechanism is particularly useful in scenarios where different spatial cell clusters exhibit varying growth rates, such as during callus formation in response to wound healing (Giannino et al., 2019), in root nodules containing nitrogen-fixing bacteria (Brewin, 2004), and in gall formation initiated by insect activity (Takeda et al., 2021).

Refined cell wall mechanics

Cell walls play an integral role in plant morphology and development: plant tissues are composed of cells of various ages and cell types that fulfil very different roles for plant survival. Younger cells tend to have only a flexible and relatively permeable primary cell wall, allowing for growth and expansion, while older cells that have already differentiated to their definitive role will have a more stable and rigid secondary cell wall. Depending on the cell type, these secondary cell walls can be further differentiated, e.g. in secondary wall patterning during xylem differentiation (Oda and Fukuda, 2012). We implemented an improved representation of cell wall stiffness to enable VirtualLeaf to manage detailed plant wall dynamics. Cell wall stiffness can now be differentiated on a per-cell basis, allowing for a more realistic tissue representation during simulations, see **cell-2** and **cell-3** in Fig. 5a.

By defining *wall element*-specific stiffness $w(j)$, we can now describe anisotropies in cell wall structures on the level of a single cell, such as **cell-1** in Fig. 5a: The shaded top and bottom cell wall elements have different stiffness values than the vertical ones. During simulations, the specific stiffness for this wall element is integrated into the Hamiltonian; the base cell-specific value applies to the wall elements where no additional stiffness was defined Fig. 5b. We further refined the cell wall relaxation behaviour, calculating the Hamiltonian independent of the *target length* using a similar approach to Dzhurakhalov et al. (2012): Instead of the *target length* or the base length of the entire wall (Dzhurakhalov et al., 2012; Dzhurakhalov, 2015) we use the base length $B(j)$ of the wall element, i.e. the length of the element at rest without any forces acting on it, to calculate the wall element's contribution to the Hamiltonian. In the Hamiltonian H_L itself, we use the degree of stretching to asses the energy in the system:

$$e = \frac{L(j) - B(j)}{B(j)}. \tag{6}$$

Therefore, the cell wall component of the Hamiltonian is now composed of λ_L (the general scaling factor for all cell walls), E (representing the elastic modulus of the tissue), the base length $B(j)$, $w(j)$ (the wall element-specific stiffness) and $(e(j)_t - e(j))^2$ (the squared difference of the stretched positions of the cell wall element).

$$H_\mathrm{L} = \lambda_L \; E \; \Sigma_j \; B(j) \; w(j) \; (e(j)_t - e(j))^2. \tag{7}$$

The fundamental principle remains unchanged: cell wall elements are described as springs being stretched (or compressed) throughout simulations. The newly introduced aspect is that this calculation became independent of the target length and instead refers to the base length of the wall element. The deformation is assumed to be elastic for an extension of the wall element to up to 20%, similar to the approach taken by Dzhurakhalov (2015). Beyond this point, experiments demonstrate cellulose fibres transition from elastic to plastic behaviour (i.e., they irreversibly deform). We represent this transition by updating the wall element's base length if it extends more than 20%. Although we have removed the target distance between nodes (target length) from the cell wall's contribution to the Hamiltonian, introducing

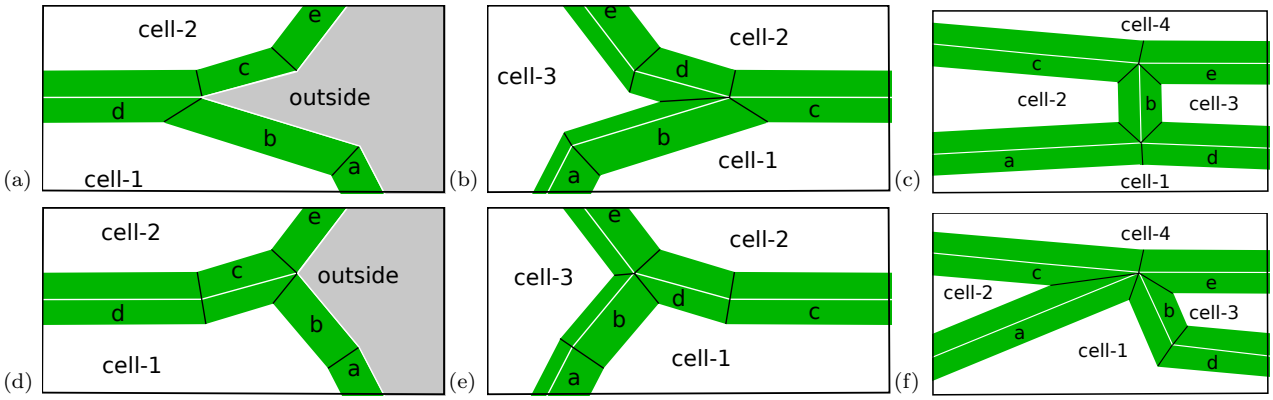

Fig. 3: The representation of the behaviour of the wall elements between the cells in case of squished edges. (a) During the growth of two neighbouring border cells, the closing of the space between **b** and **c** is imminent. (d) Moving the wall-element **b** from the intersection between **d** and **c** to the intersection between **c** and **e** benefits the energetic equilibrium. (b) The **cell-3** is compressed between **cell-1** and **cell-2**, forcing the cell wall elements into a sharp angle (between **b** and **d**). (e) VirtualLeaf will move the wall between the lower and left cell (between **d** and **e**) to reduce the tension on the cell wall. (c) Cell compression on a wall element intersection will be detected by evaluating the remodelling Hamiltonian between **a** and **c** assuming the **b** wall removed. (f) The **cell-1** is exerting pressure on the thin and stretched **cell-2** and **cell-3**. The compression is relieved by the same algorithm as in (e) and (d), resulting in remodelling the wall-element **a** to the intersection of **b** and **c**.

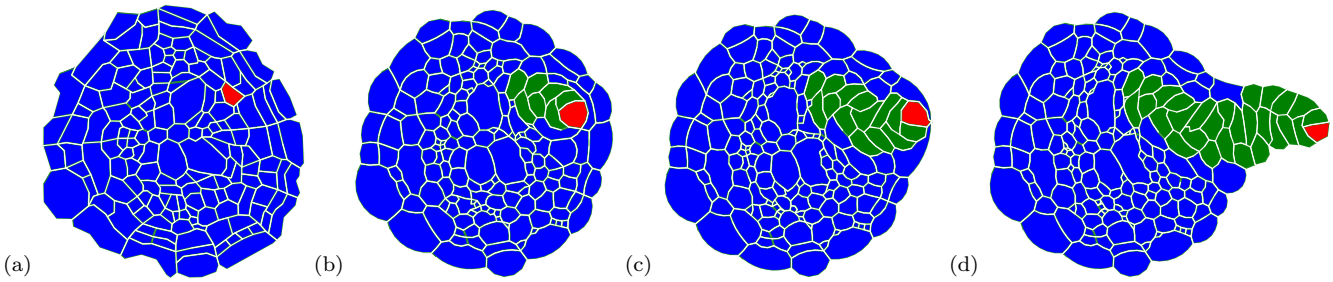

Fig. 4: Time-lapse visualisation of a proliferating lateral root emerging from the stationary (assumed non-growing) taproot, as depicted in Fig. 1a. The cell colour distinguishes cell types. Dynamic remodelling of wall elements facilitates the migration and expansion of growing cells through the quiescent cell population within the taproot tissue. The underlying simplified model includes only one cell undergoing growth and division. In each division, the rightmost cell is selected to grow next. The time-lapse sequence is extracted from the video in the supporting information (Section 1.2.1). (a) Initial simulation state of the quiescent tissue (refer to Fig. 1c). A single cell in the fourth cell layer is designated as the origin of the lateral root. (b) As the growing cell cluster expands, it exerts pressure on the surrounding quiescent tissue. (c) The expanding cell cluster reaches the boundary of the tissue. (d) Remodelling of wall elements facilitates the lateral root's growth through the stem wall, allowing it to emerge outside the taproot.

new nodes still depends on the overall length of a wall element exceeding the threshold, a behaviour compatible with the previous releases of VirtualLeaf.

New research direction: mechanical effects of pathogen infection

The Refined cell wall mechanics of VirtualLeaf opens up several new research directions where a more detailed mechanical description is necessary, e.g. during pathogen infection. Pathogens utilise various strategies to weaken the plant cell wall during infection. For instance, fungal necrotrophs extensively degrade the cell wall using degrading enzymes, while biotrophic fungi employ a more controlled degradation to keep host cells alive (Bellincampi et al., 2014). Additionally, phytopathogenic microorganisms deploy cell wall-degrading enzymes to breach the plant cell wall barrier, facilitating infection (Cooper, 1989). The presented version of VirtualLeaf is able to simulate these cell wall infection dynamics. To illustrate this, we built a simplified model of infection dynamics over a small tissue region (see Fig. 6a to Fig. 6d and Section 1.2.1), which was generated using the SVG translator (see 1f). Here, one foreign cell (e.g. a fungi) starts growing at the outside of the tissue. Through the release of cell wall destabilising components, the cell walls of the plant cells are slowly weakened (as illustrated by the decreasing line thickness) until the pathogen can infiltrate the plant tissue.

New implementation of cell wall dynamics is compatible with older models

While we sought to improve cell wall mechanics in VirtualLeaf, we also wanted to ensure the compatibility of this updated version of VirtualLeaf with models built using previous versions of VirtualLeaf. As such, the default parameters of all cell wall

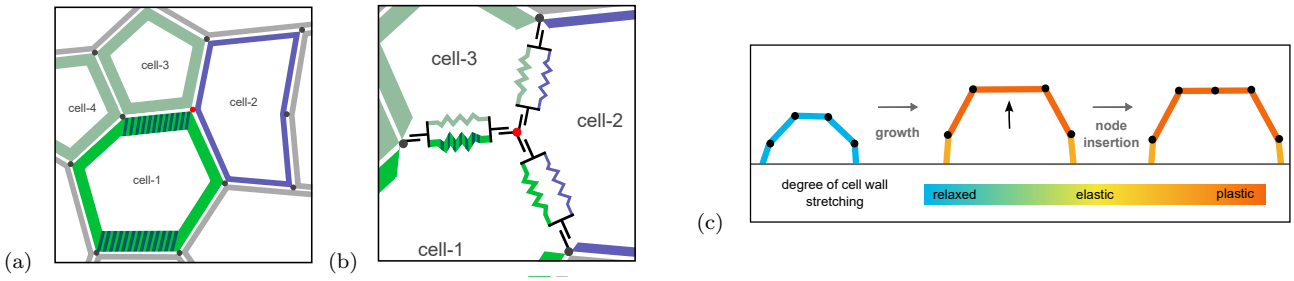

Fig. 5: Refined cell wall mechanics in VirtualLeaf. (a). Cells can now have cell-specific wall stiffness values as indicated by the line thickness and colour of **cell-1** to **cell-4**. Additionally, cells can also have anisotropic wall stiffness values as indicated by the shaded wall elements of **cell-1**. (b) VirtualLeaf will take into account the stiffness values for all cell elements connected to a node when evaluating the change in the Hamiltonian during tissue simulations. (c) The introduction of new nodes, no longer results in the relaxation of cell wall elements. The two new wall elements will remain under tension maintaining the tissue layout (Michels et al., 2020).

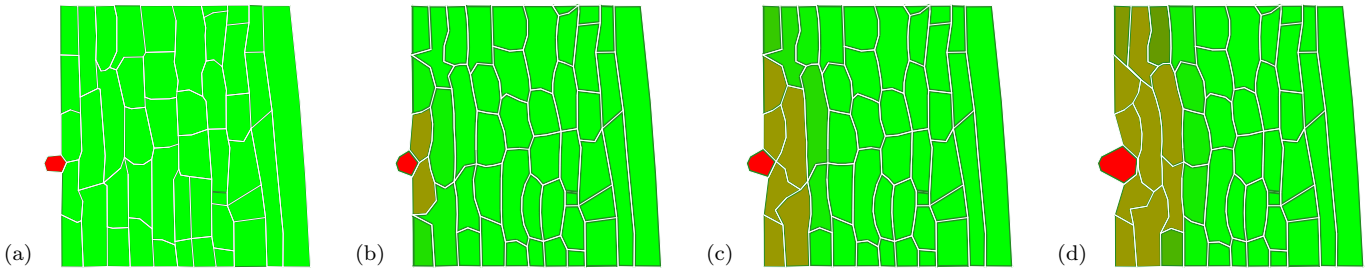

Fig. 6: Time-lapse visualisation depicting a pathogen compromising tissue integrity. The pathogen initially sits at the outside of the tissue (a). As the pathogen grows, it exudes a cell wall weakening chemical ((b) and (c), shown in brown), weakening the cell walls and destabilising the tissue. This allows the pathogen to infiltrate the plant tissue (d).

stability values were set such that the tissue dynamics simulations of older models were unchanged. We verified this behaviour by comparing the simulation results between VirtualLeaf v2 and the one with the changed cell wall dynamics. In particular, we repeated the simulations ten times for both software versions and compared the respective cell counts and area values. Neither the cell count nor the cell area showed a significant difference between simulations based on a Kolmogorov-Smirnov test (cell count: p-value = 0.142; cell area: p-value = 0.398).

Discussion

Computational models have become an indispensable tool in biological research to contextualise and analyse biological systems (Hübner et al., 2011; Holzheu and Kummer, 2019; **?**). With the increasing prevalence of computational models, however, the need for continuous method and tool development continues to open up new research questions: COPASI for models consisting of ordinary differential equations (Hoops et al., 2006) paving the way for highly complex biochemical network simulations, spatial model editor for continuous partial differential equations models, Smoldyn for discrete particle simulations to simulate spatial dynamics of e.g. spatially heterogeneous membrane environments in signalling pathways (Andrews, 2016), and SDA for to study macromolecular interactions and complex biochemical and structural biology systems (e.g. protein adsorption to surfaces, large systems with multiple solutes) (Martinez et al., 2015).

VirtualLeaf fulfils a vital role in facilitating the simulation of plant tissues (De Vos et al., 2014; Lebovka et al., 2023), particularly in areas currently inaccessible to life-cell imaging where computational modelling can provide an indication for describing the dynamics of developmental processes such as radial growth (Lebovka et al., 2023). Furthermore, it has been the starting point of several new computational approaches (Wolff et al., 2019; De Vos et al., 2017).

This study introduces an updated version of VirtualLeaf that enables a more accurate mechanical representation of plant tissues. This improvement is achieved through a more detailed and precise implementation of cell wall mechanics. More specifically, incorporating cell wall element-based properties in our modelling approach enables the accurate representation of realistic cell and tissue configurations, wherein every cell type can be accurately represented as to their cell wall properties. We have refined the cell wall contribution to the Hamiltonian by making the calculation independent of the target length similar to Dzhurakhalov et al. (2012); Dzhurakhalov (2015). By decoupling the wall energy from introducing new nodes, we allow for a more realistic simulated behaviour, capturing the elastic-plastic behaviour of cell wall filaments. Unlike the work done by Dzhurakhalov, we chose to introduce a base length for the individual wall elements instead of for the entire cell wall, in line with the wall element level of resolution of the described biomechanics.

Although cell wall stability is crucial for maintaining plant integrity, specific stages in plant development necessitate tissue morphological rearrangement and cell wall remodelling. This

morphological rearrangement is particularly evident during processes such as lateral root emergence (Stoeckle et al., 2018) and rhizobium-legume symbiosis (Brewin, 2004). Therefore, we have introduced a mechanism for cell wall remodelling in VirtualLeaf, similar to the approach taken by Wolff et al. (2019). The corresponding Hamiltonian for cell wall remodelling utilises the improved cell wall mechanics. With this formulation of the Hamiltonian, we take a slightly different approach to Wolff et al. (2019), who instead used the area conservation and the adhesion energy between cells to assess the energy of cell wall remodelling.

We have ensured compatibility with models built in previous versions of VirtualLeaf: it is still possible to load and simulate models using the previous version of the Hamiltonian. Cell wall remodelling can also be inactivated to match simulation results obtained with previous releases of VirtualLeaf.

Considering the central role of the cell wall in plant physiology and development (Sassi and Traas, 2015; Wolf, 2022), an accurate representation of the mechanical properties and behaviours of the plant cell wall is an essential step when simulating plant tissues. The refining cell wall mechanics in VirtualLeaf opened up several new research questions that can now be addressed. As exemplified in this paper, with the improved cell wall mechanics, it is in principle, possible to *i)* analyse growth effects beyond a descriptive increase in cell size and *ii)* study the potential mechanical effects of pathogen infection. The introduction of cell wall "remodelling" opens up a third research direction simulating the emergence of lateral roots and rhizobium-legume symbiosis.

While these steps represent an essential step towards accurately simulating plant tissue growth, some limitations still need to be considered. Important effects such as growth anisotropy can currently only be represented in a descriptive manner (De Vos et al., 2014), where the direction of growth is predetermined.

VirtualLeaf continues to be developed further and expanded to new research areas. We are looking to implement additional biomechanical components to support anisotropic growth, giving VirtualLeaf capabilities to simulate a more comprehensive array of biological processes to support hypothesis-driving research in plant biology.

Conclusion

The updated version of VirtualLeaf represents an essential step towards more realistic simulations of plant tissue dynamics. The increased level of detail in the description of cell wall mechanics and introduction of cell wall remodelling opens up several new research areas that can be studied using VirtualLeaf models, e.g. the mechanical effects of growth, cell wall remodelling enzymes or pathogen infections.

Supporting information

Video and Image generation.
VirtualLeaf generates PDF images at regular intervals during the simulation. These images were converted using the "convert" image conversion package available on Linux. Subsequently, the sequence of images was compiled into videos using the FFmpeg software. The following script was employed to automatically convert a directory of VirtualLeaf images into videos and their corresponding EPS file versions.

Listing 1. bash 5.1

```
#!/bin/bash

j=0
for i in 'leaf'*.png; do
    j=$((j + 1))
    out='test-'$(printf "%04d" $j)'.png'
    convert -density 300 -trim -resize 1024x790 \
      -background White -gravity center \
      -extent 1024x790 $i $out
done
j=0
for i in 'leaf'*.pdf; do
    j=$((j + 1))
    out='test-'$(printf "%04d" $j)'.eps'
    pdfcrop $i cropped.pdf
    pdftops -eps cropped.pdf $out
    rm cropped.pdf
done
ffmpeg -framerate 5 -i test-%04d.png \
   -c:v libx264 -r 30 -pix_fmt yuv420p out.mp4
```

S1 Video.

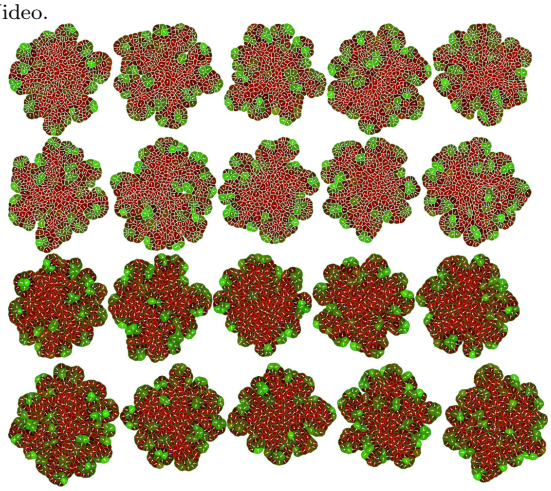

10 times random growth of the auxin model updated version followed 10 times random growth of the auxin model in the previous version.

S2 Video.

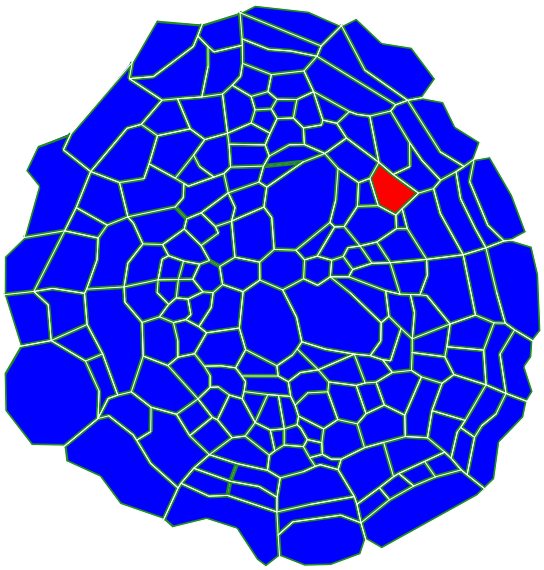

Growth dynamics during lateral root initiation including cell wall loosening.

S3 Video.

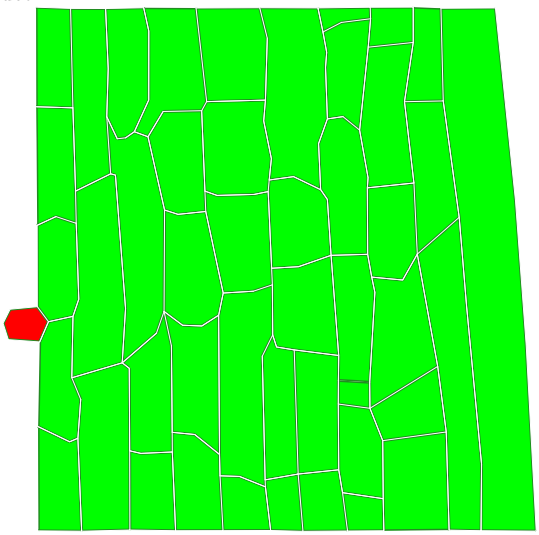

Pathogen growth and cell wall weakening effects in VirtualLeaf.

Python Script Instructions

This updated release of VirtualLeaf includes a Python script that allows for a more straightforward translation of plant tissues to simulation templates called leaves in VirtualLeaf. However, these templates are versatile and can be applied to various plant structures beyond leaves. We provide a detailed step-by-step introduction to the script and the generation of the scalable vector graphics (SVG) files the script uses.

Prerequisites

For the script to function properly, it is imperative that both Python 3.10 (Van Rossum and Drake Jr, 1995) and Inkscape (Harrington, 2004-2005) are available on the machine. Additionally, the script requires the python packages shapely (1.8.0) and sympy (1.9) to function properly.

Generating the SVG File

In this step, a microscopy image is used as a template to create an SVG file of the same tissue, which will then be inserted into an XML template by the Python script. The basic idea is to create a path of freehand lines in Inkscape for each cell's circumference. By defining the boundaries, we obtain points that uniquely identify each cell. The Python script can then translate these points into a set of nodes for each cell. At this stage, we can already define various cell types by assigning each type a specific colour, e.g., all epidermis cells are red, and all xylem cells are blue. Note: The fixed cells have a predefined colour in the script (black). Although this can be adjusted, we suggest outlining the fixed cells of the tissue in black for simplicity's sake.

Considering the minimal tissue in **??**, all cells in the tissue template need to be traced using a closed path. To do this, select the pen tool (for curved and straight lines) in Inkscape and mark every critical point around the tissue. As these points will later be translated to node coordinates, all essential points of all cells need to be considered during this process. It is crucial to ensure that the path starts and ends at the same point - Inkscape will recognise the closed shape, which is necessary for cell identification later in the process. By tracing all cells belonging to the same cell type using the same colour, the cell type can already be predefined at this stage. In the example tissue, **cell-1**, **cell-2**, and **cell-4** have the same cell type and are therefore outlined in the same colour (blue). **Cell-3** belongs to a different cell type and is therefore outlined in red. During the tracing process, the essential points for that cell but also those of the neighbouring cells need to be considered: While the green node in **??** is not necessary for **cell-1**, it is essential for defining the border between **cell-2** and **cell-4** and must be included in the outline of all three cells. Furthermore, the shared points between cells must be identical or at least very close together to be recognised as one node. Otherwise, a situation will occur, such as with **cell-3** in Fig. **??**, where there is a gap in the tissue. This erroneous gap will result in a small erroneous cell being defined in the translation process.

Running the script

The script facilitates the customisation of multiple parameters, including the designation and directory of the template file, which outlines the overarching structure and general parameters for the XML file alongside the desired filename for the resulting XML document. Additionally, users can specify a scaling factor to appropriately map x and y coordinates to the cellular scale and a colour map for encoding cell types within the SVG file. Furthermore, specific details for each cell type are provided, delineated by colons and their hex colour code, encompassing elements such as cell type and intracellular chemical concentrations.

python readsvg.py -i "path to the SVG file (without .svg)" -t "path to the XML template file (with file extension)" -s "numerical scaling factor between image and simulation template" -c "color code"

The colour code has the form of "RGB colour code, cell type, intracellular species concentrations: RGB colour code, cell type, intracellular species: ... : ... :" until all colour codes are described.

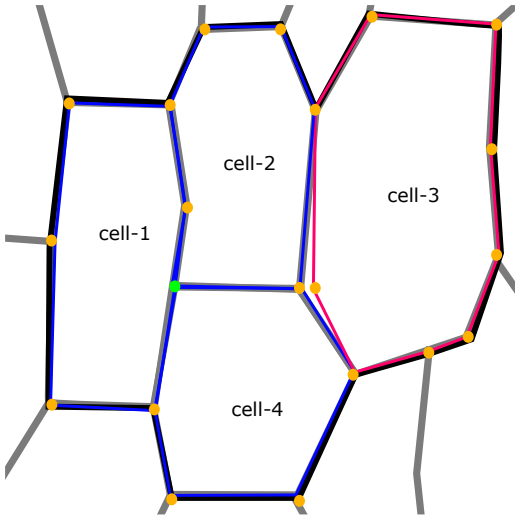

Fig. 7: Generating an SVG template file for the Python script requires careful tracing of the tissue outline. Several constellations can cause issues in the translation from SVG to XML: While tracing the microscopy image, special care should be taken to include all essential points. While the highlighted green node might not be required for the outline of **cell-1**, it is necessary to define the boundary between cell-2 and **cell-4** and should, therefore, also be included in the outline of **cell-1**. Furthermore, the corner points must be close together for neighbouring cells to be recognised as one node. Otherwise, a double node situation occurs, as illustrated in **cell-3**.

Control of Features

To ensure seamless compatibility with prior versions of VirtualLeaf, we have implemented an augmented parameter named "compatibility_level" within the option framework. This parameter operates as a bit flag; additional features are (de)activated by (re)setting the bit value in the "compatibility_level" unsigned 16-bit integer value. This "compatibility_level" also facilitates the seamless integration of forthcoming enhancements. The "WALL STIFFNESS HAMILTONIAN" constant is represented by the value "1" (corresponding to the bit value "0x0001"), while the "WALL SLIDING" corresponds to "3" (bit value "0x0003". The wall sliding functionality necessitates the activation of wall stiffness. The default value is presently set at "65535" (corresponding to a bit value of "0xFFFF"), thereby ensuring the activation of supplementary future features.

Example Simulations

Infection model

For this simple infection model, we use the tissue template presented in 1f, adding a pathogenic cell (e.g., a fungal cell) outside the tissue. The outside boundaries of this tissue are fixed to maintain the overall tissue shape, and all remaining nodes can move according to the tissue energy. The pathogenic cell secretes a chemical factor that diffuses throughout the tissue and degrades cell wall stability, while plant cells degrade this chemical at a rate of k. The pathogenic cell will grow and use the destabilised cell walls to grow into the plant tissue.

The intracellular model only considers the dynamics of the pathogenic chemicals. In the pathogen, we assume a constant chemical level for simplicity's sake. For plant cells, the actual chemical levels will depend on the diffusion and the degradation within the cell:

$$\frac{d[X]}{dt} = scaled\,diffusion \cdot D \cdot \Delta[X] - k \cdot [X]$$

Scaling factor for pathogenic chemical diffusion

In the equations describing the pathogen diffusion from one cell to the next, we have included a scaling factor for the pathogen concentration changes in **cell-1** and **cell-2**. To ensure mass conservation, we require that the total amount of pathogen remains constant:

$$n \cdot (pathogen_{cell-1}) + n \cdot (pathogen_{cell-2}) = constant \tag{8}$$

and as a consequence

$$\frac{dn_1}{dt} + \frac{dn_2}{dt} = 0 \tag{9}$$

It follows that

$$\alpha \cdot V_1 \cdot \Delta C_{pathogen} = \beta \cdot V_2 \cdot \Delta C_{pathogen} \tag{10}$$

$$\Rightarrow \alpha \cdot V_1 = \beta \cdot V_2 \tag{11}$$

$$\Rightarrow \frac{\alpha}{\beta} = \frac{V_2}{V_1} \cdot \frac{V_{tot}}{V_{tot}} \tag{12}$$

with V_{tot} being the sum of V_1 and V_2. Based on the equations above, we set the scaling factors to

$$\alpha = \frac{V_2}{V_{tot}}, \quad \beta = \frac{V_1}{V_{tot}} \tag{13}$$

Lateral Root Model

The simplified lateral root model begins with the imported taproot model (see Fig. 1a), where one of the cells is designated as a lateral root founder cell (cell type = 3). In this model, only the rightmost cell of cell type 3 is defined as actively growing. The cell division threshold is set to two times the average model cell area. During cell division, the rightmost daughter cell is selected to continue as the growing cell.

Source Code

The source code for VirtualLeaf is provided as a ZIP file in the supplementary materials.

For experienced users, the updated version of VirtualLeaf can be accessed using the Git version control system from the GitHub repository at `https://github.com/rmerks/VirtualLeaf2021`. The specific version used in this manuscript is tagged as Enhanced_Cell_Wall_Mechanics_in_VirtualLeaf_2024_v1.0.

Competing interests

The authors declare no conflicts of interest.

Author contributions statement

Ruth Großeholz and Richard W. van Nieuwenhoven contributed equally to the design and implementation of the research, the analysis of the results and the writing of the manuscript. Bruno Hay Mele contributed to the design of the cell-specific cell wall stiffness and reviewed the manuscript. Roeland M.H. Merks helped with the design in general and edited the manuscript.

Acknowledgements

R.G. would like to thank the CRC-1101 project D02 of the German Research Foundation and the Dutch Sectorplan 2 beta for funding and the Joachim Herz Foundation for its support. The authors acknowledge TU Wien Bibliothek for financial support through its Open Access Funding Programme. R.W.N. would like to acknowledge Ille C. Gebeshuber for her guidance, mentorship, academic insights and support, which have been invaluable throughout this research project. R.W.N. extends his gratitude to Fabian Buranits for his assistance in identifying Hamiltonian and programming problems during this research; his contribution and dedication to the project have been greatly appreciated. R.M.H.M. was supported by NWO grant NWO/ENW-VICI 865.17.004 and by the Prof. Dr. Jan van der Hoevenstichting voor Theoretische Biologie affiliated to the Leiden University Fund (LUF).

References

S. S. Andrews. Smoldyn: particle-based simulation with rule-based modeling, improved molecular interaction and a library interface. *Bioinformatics*, 33(5):710–717, Dec. 2016. ISSN 1367-4811. doi: 10.1093/bioinformatics/btw700. URL `http://dx.doi.org/10.1093/bioinformatics/btw700`.

C.-C. Antonovici, G. Y. Peerdeman, H. B. Wolff, and R. M. H. Merks. *Modeling Plant Tissue Development Using VirtualLeaf*, page 165–198. Springer New York, Nov. 2021. ISBN 9781071618165. doi: 10.1007/978-1-0716-1816-5_9. URL `http://dx.doi.org/10.1007/978-1-0716-1816-5_9`.

D. Bellincampi, F. Cervone, and V. Lionetti. Plant cell wall dynamics and wall-related susceptibility in plant–pathogen interactions. *Frontiers in Plant Science*, 5, May 2014. ISSN 1664-462X. doi: 10.3389/fpls.2014.00228. URL `http://dx.doi.org/10.3389/fpls.2014.00228`.

N. J. Brewin. Plant cell wall remodelling in the rhizobium–legume symbiosis. *Critical Reviews in Plant Sciences*, 23(4):293–316, July 2004. ISSN 1549-7836. doi: 10.1080/07352680490480734. URL `http://dx.doi.org/10.1080/07352680490480734`.

K. Caesar, K. Elgass, Z. Chen, P. Huppenberger, J. Witthöft, F. Schleifenbaum, M. R. Blatt, C. Oecking, and K. Harter. A fast brassinolide-regulated response pathway in the plasma membrane of arabidopsis thaliana. *The Plant Journal*, 66(3): 528–540, 2011. doi: 10.1111/j.1365-313X.2011.04510.x. URL `http://dx.doi.org/10.1111/j.1365-313X.2011.04510.x`.

V. Chickarmane, A. H. Roeder, P. T. Tarr, A. Cunha, C. Tobin, and E. M. Meyerowitz. Computational morphodynamics: A modeling framework to understand plant growth. *Annual Review of Plant Biology*, 61(1):65–87, June 2010. ISSN 1545-2123. doi: 10.1146/annurev-arplant-042809-112213. URL `http://dx.doi.org/10.1146/annurev-arplant-042809-112213`.

R. M. Cooper. *Host Cell Wall Loosening and Separation by Plant Pathogens*, page 165–178. Springer Berlin Heidelberg, 1989. ISBN 9783642741616. doi: 10.1007/978-3-642-74161-6_16. URL `http://dx.doi.org/10.1007/978-3-642-74161-6_16`.

D. J. Cosgrove. Assembly and enlargement of the primary cell wall in plants. *Annual review of cell and developmental biology*, 13 (1):171–201, 1997.

D. De Vos, K. Vissenberg, J. Broeckhove, and G. T. S. Beemster. Putting theory to the test: Which regulatory mechanisms can drive realistic growth of a root? *PLoS Computational Biology*, 10(10):e1003910, Oct. 2014. ISSN 1553-7358. doi: 10.1371/journal.pcbi.1003910. URL `http://dx.doi.org/10.1371/journal.pcbi.1003910`.

D. De Vos, A. Dzhurakhalov, S. Stijven, P. Klosiewicz, G. T. S. Beemster, and J. Broeckhove. Virtual plant tissue: Building blocks for next-generation plant growth simulation. *Frontiers in Plant Science*, 8, May 2017. ISSN 1664-462X. doi: 10.3389/fpls.2017.00686. URL `http://dx.doi.org/10.3389/fpls.2017.00686`.

A. Dzhurakhalov. *Modelling plant cell expansion in VirtualLeaf*. PhD thesis, Universiteit Antwerpen, 2015. URL `https://hdl.handle.net/10067/1263410151162165141`.

A. Dzhurakhalov, D. De Vos, W. Vanroose, G. Beemster, and J. Broeckhove. Implementation of realistic cell wall mechanics in virtualleaf. In *7th Proceeding of the Plant Biomechanics International Conference. 7th Plant Biomechanics International Conference*, 2012. URL `https://hdl.handle.net/10067/1065260151162165141`.

G. Freshour, R. P. Clay, M. S. Fuller, P. Albersheim, A. G. Darvill, and M. G. Hahn. Developmental and tissue-specific structural alterations of the cell-wall polysaccharides of arabidopsis thaliana roots. *Plant physiology*, 110(4):1413–1429, 1996. doi: 10.1104/pp.110.4.1413. URL `http://dx.doi.org/10.1104/pp.110.4.1413`.

H. L. Gall, F. Philippe, J.-M. Domon, F. Gillet, J. Pelloux, and C. Rayon. Cell wall metabolism in response to abiotic stress. *Plants*, 4(1):112–166, 2015.

A. Ghaffarizadeh, R. Heiland, S. H. Friedman, S. M. Mumenthaler, and P. Macklin. Physicell: An open source physics-based cell simulator for 3-d multicellular systems. *PLOS Computational Biology*, 14(2):e1005991, Feb. 2018. ISSN 1553-7358. doi: 10.1371/journal.pcbi.1005991. URL `http://dx.doi.org/10.1371/journal.pcbi.1005991`.

F. Giannino, B. Hay Mele, V. De Micco, G. Toraldo, S. Mazzoleni, and F. Carteni. An individual based model of wound closure in plant stems. *IEEE Access*, 7:65821–65827, 2019. ISSN 2169-3536. doi: 10.1109/access.2019.2915575. URL `http://dx.doi.org/10.1109/ACCESS.2019.2915575`.

R. Großeholz, F. Wanke, L. Rohr, N. Glöckner, L. Rausch, S. Scholl, E. Scacchi, A.-J. Spazierer, L. Shabala, S. Shabala, K. Schumacher, U. Kummer, and K. Harter. Computational modeling and quantitative physiology reveal central parameters for brassinosteroid-regulated early cell physiological processes linked to elongation growth of the arabidopsis root. *eLife*, 11, Sept. 2022. ISSN 2050-084X. doi: 10.7554/elife.73031. URL `http://dx.doi.org/10.7554/eLife.73031`.

A. Hager, H. Menzel, and A. Krauss. Versuche und hypothese zur primärwirkung des auxins beim streckungswachstum. *Planta*, 100(1):47–75, 1971. doi: 10.1007/BF00386886. URL `https://doi.org/10.1007/BF00386886`.

A. Hager, G. Debus, H. Edel, H. Stransky, and R. Serrano. Auxin induces exocytosis and the rapid synthesis of a high-turnover pool of plasma-membrane h+-atpase. *Planta*, 185(4):527–537,

1991. doi: 10.1007/BF00202963. URL https://doi.org/10.1007/BF00202963.

B. Harrington. Inkscape, 2004-2005. URL http://www.inkscape.org.

K. Hématy, C. Cherk, and S. Somerville. Host–pathogen warfare at the plant cell wall. *Current opinion in plant biology*, 12(4): 406–413, 2009. doi: 10.1016/j.pbi.2009.06.007. URL https://doi.org/10.1016/j.pbi.2009.06.007.

P. Holzheu and U. Kummer. Computational systems biology of cellular processes in arabidopsis thaliana: an overview. *Cellular and Molecular Life Sciences*, 77(3):433–440, Nov. 2019. ISSN 1420-9071. doi: 10.1007/s00018-019-03379-9. URL http://dx.doi.org/10.1007/s00018-019-03379-9.

P. Holzheu, M. Krebs, C. Larasati, K. Schumacher, and U. Kummer. An integrative view on vacuolar ph homeostasis in arabidopsis thaliana: Combining mathematical modeling and experimentation. *The Plant Journal*, 106(6):1541–1556, May 2021. ISSN 1365-313X. doi: 10.1111/tpj.15251. URL http://dx.doi.org/10.1111/tpj.15251.

S. Hoops, S. Sahle, R. Gauges, C. Lee, J. Pahle, N. Simus, M. Singhal, L. Xu, P. Mendes, and U. Kummer. Copasi—a complex pathway simulator. *Bioinformatics*, 22(24):3067–3074, Oct. 2006. ISSN 1367-4803. doi: 10.1093/bioinformatics/btl485. URL http://dx.doi.org/10.1093/bioinformatics/btl485.

K. Hübner, S. Sahle, and U. Kummer. Applications and trends in systems biology in biochemistry. *The FEBS Journal*, 278 (16):2767–2857, July 2011. ISSN 1742-4658. doi: 10.1111/j.1742-4658.2011.08217.x. URL http://dx.doi.org/10.1111/j.1742-4658.2011.08217.x.

M. Ikeuchi, K. Sugimoto, and A. Iwase. Plant callus: Mechanisms of induction and repression. *The Plant Cell*, 25(9):3159–3173, Sept. 2013. ISSN 1532-298X. doi: 10.1105/tpc.113.116053. URL http://dx.doi.org/10.1105/tpc.113.116053.

C. P. Kubicek, T. L. Starr, and N. L. Glass. Plant cell wall–degrading enzymes and their secretion in plant-pathogenic fungi. *Annual Review of Phytopathology*, 52 (1):427–451, Aug. 2014. ISSN 1545-2107. doi: 10.1146/annurev-phyto-102313-045831. URL http://dx.doi.org/10.1146/annurev-phyto-102313-045831.

I. Lebovka, B. Hay Mele, X. Liu, A. Zakieva, T. Schlamp, N. R. Gursanscky, R. M. Merks, R. Großeholz, and T. Greb. Computational modeling of cambium activity provides a regulatory framework for simulating radial plant growth. *eLife*, 12, Mar. 2023. ISSN 2050-084X. doi: 10.7554/elife.66627. URL http://dx.doi.org/10.7554/eLife.66627.

Z. Li, A. R. Fernie, and S. Persson. Transition of primary to secondary cell wall synthesis. *Science Bulletin*, 61(11):838–846, 2016. doi: 10.1007/s11434-016-1061-7. URL https://doi.org/10.1007/s11434-016-1061-7.

R. Mäkilä, B. Wybouw, O. Smetana, L. Vainio, A. Solé-Gil, M. Lyu, L. Ye, X. Wang, R. Siligato, M. K. Jenness, A. S. Murphy, and A. P. Mähönen. Gibberellins promote polar auxin transport to regulate stem cell fate decisions in cambium. *Nature Plants*, 9(4):631–644, Mar. 2023. ISSN 2055-0278. doi: 10.1038/s41477-023-01360-w. URL http://dx.doi.org/10.1038/s41477-023-01360-w.

M. Martinez, N. J. Bruce, J. Romanowska, D. B. Kokh, M. Ozboyaci, X. Yu, M. A. Öztürk, S. Richter, and R. C. Wade. ¡scp¿sda¡/scp¿ 7: A modular and parallel implementation of the simulation of diffusional association software. *Journal of Computational Chemistry*, 36(21):1631–1645, June 2015. ISSN 1096-987X. doi: 10.1002/jcc.23971. URL http://dx.doi.org/10.1002/jcc.23971.

S. McQueen-Mason, D. M. Durachko, and D. J. Cosgrove. Two endogenous proteins that induce cell wall extension in plants. *The Plant Cell*, 4(11):1425–1433, 1992. doi: 10.1105/tpc.4.11.1425. URL https://doi.org/10.1105/tpc.4.11.1425.

R. M. Merks and J. A. Glazier. A cell-centered approach to developmental biology. *Physica A: Statistical Mechanics and its Applications*, 352(1):113–130, July 2005. ISSN 0378-4371. doi: 10.1016/j.physa.2004.12.028. URL http://dx.doi.org/10.1016/j.physa.2004.12.028.

R. M. Merks, M. Guravage, D. Inzé, and G. T. Beemster. Virtualleaf: an open-source framework for cell-based modeling of plant tissue growth and development. *Plant physiology*, 155 (2):656–666, 2011. doi: 10.1104/pp.110.167619. URL https://doi.org/10.1104/pp.110.167619.

L. Michels, V. Gorelova, Y. Harnvanichvech, J. W. Borst, B. Albada, D. Weijers, and J. Sprakel. Complete microviscosity maps of living plant cells and tissues with a toolbox of targeting mechanoprobes. *Proceedings of the National Academy of Sciences*, 117(30):18110–18118, July 2020. ISSN 1091-6490. doi: 10.1073/pnas.1921374117. URL http://dx.doi.org/10.1073/pnas.1921374117.

Y. Oda and H. Fukuda. Secondary cell wall patterning during xylem differentiation. *Current Opinion in Plant Biology*, 15(1): 38–44, Feb. 2012. ISSN 1369-5266. doi: 10.1016/j.pbi.2011.10.005. URL http://dx.doi.org/10.1016/j.pbi.2011.10.005.

Y. B. Park and D. J. Cosgrove. Changes in cell wall biomechanical properties in the xyloglucan-deficient xxt1/xxt2 mutant of arabidopsis. *Plant physiology*, 158(1):465–475, 2012. doi: 10.1104/pp.111.189779. URL https://doi.org/10.1104/pp.111.189779.

K. M. Rai, V. K. Balasubramanian, C. M. Welker, M. Pang, M. M. Hii, and V. Mendu. Genome wide comprehensive analysis and web resource development on cell wall degrading enzymes from phyto-parasitic nematodes. *BMC Plant Biology*, 15(1), Aug. 2015. ISSN 1471-2229. doi: 10.1186/s12870-015-0576-4. URL http://dx.doi.org/10.1186/s12870-015-0576-4.

Y. Rui and J. R. Dinneny. A wall with integrity: surveillance and maintenance of the plant cell wall under stress. *New Phytologist*, 225(4):1428–1439, Sept. 2019. ISSN 1469-8137. doi: 10.1111/nph.16166. URL http://dx.doi.org/10.1111/nph.16166.

J. P. Rutten and K. ten Tusscher. In silico roots: Room for growth. *Trends in Plant Science*, 24(3):250–262, Mar. 2019. ISSN 1360-1385. doi: 10.1016/j.tplants.2018.11.005. URL http://dx.doi.org/10.1016/j.tplants.2018.11.005.

M. Sassi and J. Traas. When biochemistry meets mechanics: a systems view of growth control in plants. *Current Opinion in Plant Biology*, 28:137–143, Dec. 2015. ISSN 1369-5266. doi: 10.1016/j.pbi.2015.10.005. URL http://dx.doi.org/10.1016/j.pbi.2015.10.005.

T. Y. Shcherban, J. Shi, D. M. Durachko, M. J. Guiltinan, S. J. McQueen-Mason, M. Shieh, and D. J. Cosgrove. Molecular cloning and sequence analysis of expansins–a highly conserved, multigene family of proteins that mediate cell wall extension in plants. *Proceedings of the National Academy of Sciences*, 92(20):9245–9249, 1995. doi: 10.1073/pnas.92.20.9245. URL https://doi.org/10.1073/pnas.92.20.9245.

J. Starruß, W. de Back, L. Brusch, and A. Deutsch. Morpheus: a user-friendly modeling environment for multiscale and multicellular systems biology. *Bioinformatics*, 30(9):1331–1332,

Jan. 2014. ISSN 1367-4803. doi: 10.1093/bioinformatics/btt772. URL http://dx.doi.org/10.1093/bioinformatics/btt772.

D. Stoeckle, M. Thellmann, and J. E. Vermeer. Breakout — lateral root emergence in arabidopsis thaliana. *Current Opinion in Plant Biology*, 41:67–72, Feb. 2018. ISSN 1369-5266. doi: 10.1016/j.pbi.2017.09.005. URL http://dx.doi.org/10.1016/j.pbi.2017.09.005.

M. H. Swat, G. L. Thomas, J. M. Belmonte, A. Shirinifard, D. Hmeljak, and J. A. Glazier. *Multi-Scale Modeling of Tissues Using CompuCell3D*, page 325–366. Elsevier, 2012. doi: 10.1016/b978-0-12-388403-9.00013-8. URL http://dx.doi.org/10.1016/B978-0-12-388403-9.00013-8.

S. Takeda, T. Hirano, I. Ohshima, and M. H. Sato. Recent progress regarding the molecular aspects of insect gall formation. *International Journal of Molecular Sciences*, 22(17):9424, Aug. 2021. ISSN 1422-0067. doi: 10.3390/ijms22179424. URL http://dx.doi.org/10.3390/ijms22179424.

W. Underwood. The plant cell wall: a dynamic barrier against pathogen invasion. *Frontiers in plant science*, 3:85, 2012. doi: 10.3389/fpls.2012.00085. URL https://doi.org/10.3389/fpls.2012.00085.

S. van Mourik, K. Kaufmann, A. D. J. van Dijk, G. C. Angenent, R. M. H. Merks, and J. Molenaar. Simulation of organ patterning on the floral meristem using a polar auxin transport model. *PLoS ONE*, 7(1):e28762, Jan. 2012. ISSN 1932-6203. doi: 10.1371/journal.pone.0028762. URL http://dx.doi.org/10.1371/journal.pone.0028762.

G. Van Rossum and F. L. Drake Jr. *Python tutorial*. Centrum voor Wiskunde en Informatica Amsterdam, The Netherlands, 1995. URL https://www.python.org/.

C. Verna, S. J. Ravichandran, M. G. Sawchuk, N. M. Linh, and E. Scarpella. Coordination of tissue cell polarity by auxin transport and signaling. *eLife*, 8, Dec. 2019. ISSN 2050-084X. doi: 10.7554/elife.51061. URL http://dx.doi.org/10.7554/eLife.51061.

S. Wolf. Cell wall signaling in plant development and defense. *Annual Review of Plant Biology*, 73 (1):323–353, May 2022. ISSN 1545-2123. doi: 10.1146/annurev-arplant-102820-095312. URL http://dx.doi.org/10.1146/annurev-arplant-102820-095312.

S. Wolf, K. Hématy, and H. Höfte. Growth control and cell wall signaling in plants. *Annual Review of Plant Biology*, 63(1):381–407, June 2012. ISSN 1545-2123. doi: 10.1146/annurev-arplant-042811-105449. URL http://dx.doi.org/10.1146/annurev-arplant-042811-105449.

H. B. Wolff, L. A. Davidson, and R. M. H. Merks. Adapting a plant tissue model to animal development: Introducing cell sliding into virtualleaf. *Bulletin of Mathematical Biology*, 81(8):3322–3341, Mar. 2019. ISSN 1522-9602. doi: 10.1007/s11538-019-00599-9. URL http://dx.doi.org/10.1007/s11538-019-00599-9.

Y. Xu, C. Liu, H. Lin, K. Wang, and Z. Han. Development of the vascular cambium of taxodium ascendens and its seasonal activities in subtropical china. *Forests*, 14(6):1071, May 2023. ISSN 1999-4907. doi: 10.3390/f14061071. URL http://dx.doi.org/10.3390/f14061071.